

# Analysis of SAR interferometry for tree height estimation over hilly forested area

Thierry CASTEL<sup>§</sup>, André BEAUDOIN<sup>\*</sup> and Gérard TROUCHE<sup>§</sup>

<sup>§</sup> Unité Milieu Physique et Environnement, ENESAD, - 26, Bd Dr. Petitjean - BP 87999, France

<sup>\*</sup> Defence Research Establishment Valcartier Space Optronics Section, Data Exploitation Group 2459 PIE-XI North Blvd, Val-Bélair, Canada

---

Evaluation of current and future Synthetic Aperture Radar (SAR) data to extract forest attributes over various sites is needed. This study focuses on hilly forested man-managed pine plantation for which the estimation of height is of primary importance. Indeed this parameter is a good indicator of the forest productivity i.e. rate of growth. Furthermore it may be used to observe how forests react to their changing environment. ERS (European Remote Sensing Satellite) differential interferogram offers a great potentiality for the retrieval of such parameters. However these data may be affected by different sources of errors. In this study a simple additive model to analyze the error on the estimation of forest height is first proposed. Next, the measured and interferometric-derived height are compared. The results show a low correlation associated with high error. The error analysis shows a good agreement between predicted and observed value especially for the residual relative height. From there, it appears that the main source of error comes from the Digital Elevation Model (DEM) uncertainty and particularly for area under forest cover. A numerical study based on the model of error shows that a low level of coherence – deccorelation effect – may be considerable. Moreover, a systematic error is related to the fact that the scattering center of the layer is not the top of the canopy. Finally, the results indicate that 1) to date, differential interferometry is far from an operational use for forest height retrieval over hilly terrain, 2) even if the total error is a mixture of various sources deccorelation as well as penetration depth effects may be strongly reduced and 3) toward application purpose, a decrease on the DEM uncertainty is needed. *Agricultura 1: 15-23 (2002)*

Key words: differential interferometry; SAR; forest; estimation; tree height; error; DEM

---

## INTRODUCTION

The last decade shows the large growing of the Synthetic Aperture Radar (SAR) systems with the delivery of new data type for the monitoring of the biosphere. Such data were applied for the study of the ocean and land area (Holmes 1992, Evans et al. 1997, Kasischke et al. 1997). Among all the potential applications, the monitoring of the environmental resources such as for example forest attributes appears one of the most interesting application (Le Toan et al. 1992, Beaudoin et al. 1994, Castel et al. 2001). Especially with the L-band low frequency SAR (Dobson et al. 1995, Ranson et al. 1995, Schmullius and Evans 1997). Indeed, the quantification of the living aboveground biomass stock is a key milestone in our meaning of the responses of the terrestrial ecosystems in changing environments. This concerns both agricultural as well as forested area. The dynamic and the management of such ecosystems have a major impact on the carbon cycle and consequently on global change. However, toward the development of operational

applications for the monitoring of terrestrial ecosystems, additional researches are needed.

The ERS SAR program, managed since 1991 by the ESA (European Space Agency) agency, offers a great opportunity for the evaluation of such data for environmental monitoring (Gens and van Genderen 1996). As far as the program will be pursue with the next launch of the ENVISAT satellite. Unfortunately, numerous previous work using ERS SAR data showed that its configuration is somewhat limited for forest applications (Dobson et al. 1992, Kasischke et al. 1994). Applications can yet be broadened significantly when repeat pass INterferometric SAR (INSAR) data are considered in addition to the usual backscattering information. In interferometry, two images are taken from different vantage points of the same area. The slight difference in the two images allows to calculate an interferogram, i.e. two images of phase and correlation respectively. From past studies (Herland 1995, Wegmüller and Werner 1995, Castel et al. 2000) it was largely proved that the correlation - called degree of coherence - as an indicator of the temporal stability of the target is efficient for discrimination, change detection and retrieval parameters of the vegetation. However, even for tandem pair, the degree of coherence is strongly affected by wind (Zebker and Villasenor 1992, Beaudoin et al. 1996a, b). Furthermore for strong slopes areas (> 15°) a rejection is needed (Castel et

---

Correspondence to: Thierry CASTEL Unité Milieu Physique et Environnement, ENESAD, - 26, Bd Dr. Petitjean - BP 87999, 21079 Dijon Cedex - France (E-mail: t.castel@enesad.fr)

al. 2000). If climatic effects may be limited with a simultaneous acquisition – see for example Shuttle Radar Topography Mapping mission (Duren et al. 1998) –, effects of strong slope are not yet taken into account in the processing chain (Wegmüller et al. 1998).

On an other hand, it has been shown that the interferometric phase, usually used to derive the terrain altitude, can also be linked to the height of the forest canopy (Hagberg et al. 1995, Ulander et al. 1995, Flourey et al. 1997). However, the potential of such new data type is far from being fully explored. From our knowledge few studies have analyzed the potential of the differential interferometric phase over hilly forested areas.

The purpose of this paper is to address the potential of the differential interferometric phase for the height characterization of a forest pine plantation of Austrian black pine located over a mountainous area. The approach consists in using multi-temporal data and a Geographic Information System (GIS) to 1) experimentally analyze the sensitivity of the interferometric phase to the forest height and 2) to conduct a theoretical analysis of the sources of errors and variability for generalization purpose. The second point leads us to develop a simple additive error model in order to explain the variability and point out the future improvement for application purpose.

The following section discuss the test site characteristics and the data of the forest height collected over the area. Afterward, INSAR data are presented. This section deals with i) the summary of the theoretical specificity of the differential interferometric, ii) the evolvement of an error model for the analyze of the various sources of error and iii) the presentation of SAR data. The next section focus on the GIS-based methodology. Finally, the results are presented in the last section, which lead us to discuss the potential and limits of such data for environmental applications.

## METHODS

### Study site

The study site is situated in the southeastern of France in the central part of the Lozère department (44°30' N and 3°30' E). The physiography of the site is characterized by large and gently limestone plateaus – 1200 m a.s.l.- intercepted by gorges with 300-500m depth and steep slopes up to 50°. The forest under study is mainly composed by a state forest covering 5400 ha and a smaller privately owned plantation covering 1200 ha (Castel 1998). The planted species is almost exclusively the Austrian black pine (*Pinus nigra nigricans host.*). The site offers both a large range of growth stages as well as topographic situations.

The data collected were entered in a GIS that includes:

- A cartographic database with the limits of the forest stands;
- Information on forest stands (age class from 0-140 years by step of 20 years);
- Measurements of forest parameters such as tree height;
- A Digital Elevation Model (DEM) from the French topographic survey (IGN) with a 50-m resolution in a Lambert III projection.

### Sampling procedure and forest attributes calculation

The estimates were obtained by performing a conventional forest ground survey: Stem volume was estimated from stem density, diameter at breast height (dbh) and tree height. The sampling strategy included parameter measurements on 10-20 circular sampling plots per stand representing 2 to 7 % of the total stand surface. The plot size was 78.5 m<sup>2</sup> and 154 m<sup>2</sup> for young (< 20 years) and old tree stands respectively. Fifty-height stands with an area more than 2 ha were sampled. Forty six stands sampled by the foresters were entered in the experiment. Concerning the height, the 3 trees nearest to the center of the plot were selected and the total height was measured. The stand mean height was then computed in a straightforward manner. For the other forest attributes the calculation procedure is describe in more details by (Castel 1998). From there it was possible to derive a relationship between height and age with a coefficient of determination R<sup>2</sup>=0.98. The relation is a simplification of the Richards-Chapman equation with two parameters following:

$$H = a \times \left[ 1 - \exp \left[ \frac{-b \times age}{a} \right] \right]^2 \quad (1)$$

where a and b are two empirical coefficients equal to 24 and 0.75 respectively. The determination of the two coefficients was carried out in an iterative fashion using a nonlinear least-squares algorithm based on the Gauss-Newton method.

Figure 1A presents the adjusted height-age curve obtained for the forest test site with the associated confidence interval at 95%. Whilst Figure 1B shows the error probability distribution for measured height – at 95 % significance level - with a theoretical pdf associated law. Here the mean is equal to 7.4 %. The results point as observed over such managed forest that height variability is quite low compared to others attributes such as dbh or density.

## INSAR: THEORETICAL SUMMARY, MODELING OF ERROR AND DATA

### Acquisition and processing

Here the most important SAR consideration is that it is a coherent imaging system. As a consequence, both amplitude and phase information in the radar echo are retained during data acquisition and processing. SAR interferometry exploits this coherence using the phase measurements to infer differential range and range change in two or more SAR images of the same surface. The main successful applications concern the estimation of the topographic height and displacements (Zebker and Goldstein 1986, Massonnet et al. 1993) from the differential range measured by two radar antennas looking at the same surface. For spacecraft the way to acquire SAR interferometric data is called the repeat-pass mode i.e. the same radar antenna observing the same ground swath at different times. In each images the measured phase at each point is equal to the sum of the propagation part – proportional to the round-trip distance – and the scattering

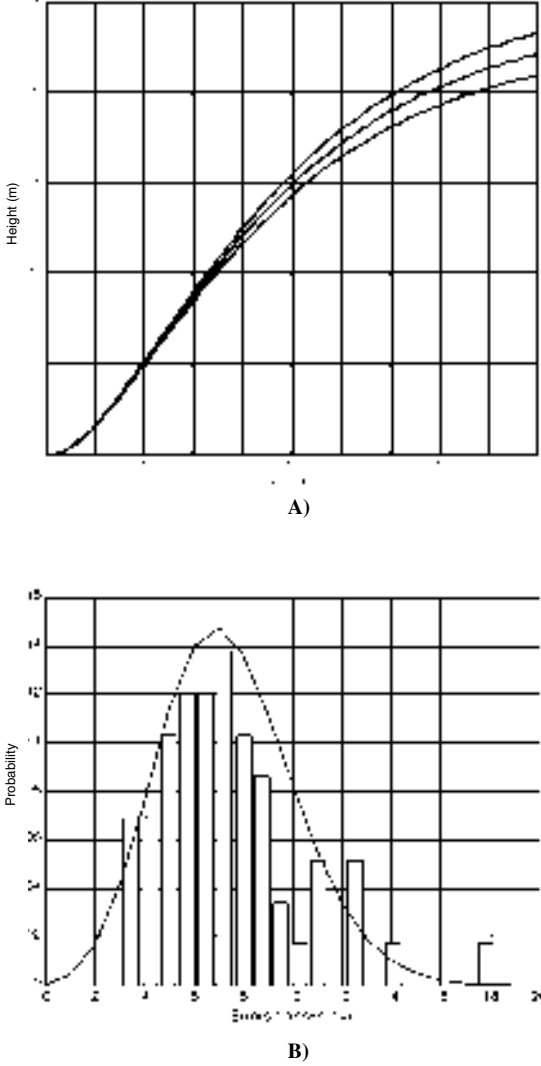


Fig. 1. A) Ajusted forest height behavior as a function of tree age. Dashed lines indicate the 95% confidence interval. B) Observed and adjusted pdf law of the errors of estimation on tree height.

part due to the interaction of the wave with the ground. Hence, if each pixel on the ground behaves the same for each observation, calculating the difference in the phases removes dependence on the scattering and gives a quantity dependent only on imaging geometry. Figure 2 presents the basic geometry for SAR interferometry. The two observations point E and M viewing the same surface with two angle  $\theta_e$  and  $\theta_m$  respectively. The positions separated by the interferometric baseline B distance with a parallel ( $B_p$ ) and a perpendicular ( $B_n$ ) components. From there the target-antenna distances  $R_e$  and  $R_m$  show difference in slant range  $\delta R$ . Hence the phase at each point is proportional to the difference in the path length  $2 \delta R$  with a constant of proportionality  $2\pi/\lambda$  following the equation:

$$\delta R = \frac{\lambda \phi}{4\pi} \quad (2)$$

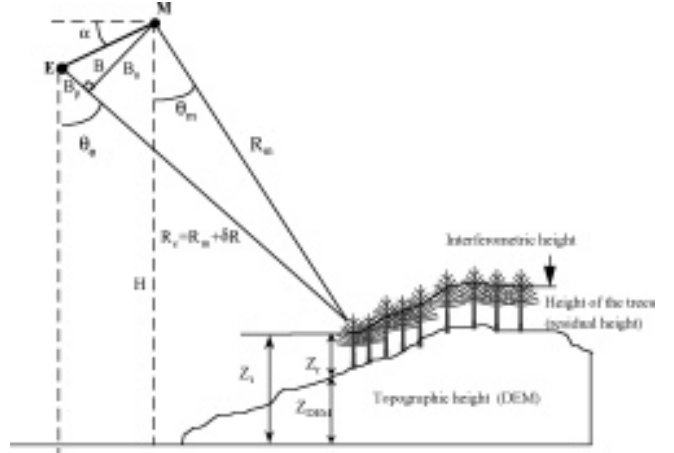


Fig. 2. General imaging geometry for SAR interferometry over an hilly forested area. M and E represent a single antenna viewing the same surface on two separate passes. In this case the two antennas both transmit and receive the radar signal.

Where  $\phi$  is the measured phase and  $\lambda$  is the wavelength. Algebra and geometry manipulation yield to the equation for height ( $Z$ ) as a function of these parameters (Zebker and Goldstein 1986).

For forested areas the signal origin from the upper part of the tree crown with a penetration depth proportional to the geometric and dielectric properties of the vegetation. Here the interferometry give us information on the topography plus the interferometric height of the tree. This height differs from the real height. The difference is low for close and dense canopy due to a lower penetration depth. This point was studied in more details by (Askne et al. 1997).

Intuitively, it may be relevant for the estimation of the tree height to derived first the height  $Z_i$  with the interferogram in order to subtract in a second step the topography given by the DEM. But as the phase is measured modulo  $2\pi$  the phase unwrapping is needed to obtain  $Z_i$  which may be problematic. To prevent that, Ulander et al. (1995) have proposed for forestry application a differential interferometry method. The method was implemented in the CNES interferometric processor (Massonnet and Rabaute 1993, Massonnet 1994) used in this work. The approach consists 1) from the DEM and a suitable knowledge of the viewing geometry to simulate the phase component due to the topography ( $\phi_{DEM}$ ), 2) to subtract to the interferogram ( $\phi$ ) the simulated phase in order to obtain the differential interferogram  $\Delta\phi$  (i.e. the residual phase). Note that  $\phi_{DEM}$  is calculated at a factor  $\text{forb}$  apart due to the systematic error on some interferometric parameters:  $B$ ,  $\theta_m$  and  $\alpha$ . As  $\Delta\phi$  is a change of the phase for a delimited area on the terrain, it may be linked to the residual altitude (i.e. height of the cover) by:

$$\Delta\phi = \phi - (\phi_{DEM} + \phi_{orb}) = \frac{Z_r}{Z_a} 2\pi \quad (3)$$

Where  $Z_i$  is the ambiguity altitude i.e. the difference of altitude that produce a variation of the phase equal to  $2\pi$ .

The estimation of the mean relative height of a forested area  $Z_{rf}$  is then possible. Nevertheless is a relative residual height because the uncertainty of the baseline subsists. Moreover, as  $Z_a$  is related to the baseline and the angle  $\alpha$  this quantity can take an infinity of values. From an operational point of view a threshold value of  $Z_a$  is needed. Indeed a decrease of  $Z_a$  related to an increase of the baseline leads to a decorrelation of the signal (Li and Goldstein 1990). Hence, a value of  $Z_a$  less than 10 m is unusable. For that, high absolute values are preferred ( $> 100$  m), unfortunately they have a low probability to occur. On the other hand, in order to obtain an accurate estimation of  $Z_{rf}$ ,  $Z_a$  must be not very high. These points lead to a compromise for the baseline values. For example (Hagberg et al. 1995) indicated an optimal range for baseline between 100 m to 300 m. However, the effect of the baseline which is unknown may be avoided with the hypothesis that it is locally constant. For that, in order to recover the absolute mean height of the forest  $Z_r$ , the derivative of the mean difference of the phase between the forested area and a close area of bared soil leads to:

$$\bar{Z}_f = \bar{Z}_{rforest} - \bar{Z}_{rsoil} = \frac{Z_a}{2\pi} (\overline{\Delta\phi}_{forest} - \overline{\Delta\phi}_{soil}) \quad (4)$$

Horizontal line denotes the average quantity. Obviously, for application purpose and following equations 3 and 4 several sources of error may affect the estimation.

### Modeling the error of estimation

It is expected that the error of estimation of both  $Z_{rf}$  and  $Z_r$  is number of independent samples, DEM quality and degree of coherence dependent. Concerning the error of estimation for the residual height relative  $\sigma_{zrf}$  and absolute  $\sigma_{zr}$ , equations 3 and 4 lead to:

$$\sigma_{zrf} = \frac{Z_a}{2\pi} \sigma_{\Delta\phi_{forest}} \quad (5)$$

and

$$\sigma_{zr} = \sqrt{\sigma_{zrf}^2 + \sigma_{zsoil}^2} = \frac{Z_a}{2\pi} \sqrt{\sigma_{\Delta\phi_{forest}}^2 + \sigma_{\Delta\phi_{soil}}^2} \quad (6)$$

with

$$\sigma_{\Delta\phi} = \sqrt{\sigma_{\phi}^2 + \sigma_{\phi_{DEM}}^2}, \text{ forest or soil} \quad (7)$$

The error of estimation of the interferometric phase  $\sigma_{\phi}$  comes from 1) the noise of the phase due to the coherence level of the target ( $\sigma_{\phi_n}$ ) and 2) the variations of the phase ( $\sigma_{\phi_z}$ ) which are the consequence of the height variations  $z$  over the viewed area  $Z$ . The noise of the phase is given by (Hagberg et al. 1995):

$$\sigma_{\phi_n} = \frac{1}{2N} \frac{\sqrt{1-\gamma^2}}{\gamma} \quad (8)$$

where  $\gamma$  is the coherence of the target between the two dates of acquisition. This noise is a function of both the number of independent sample and the degree of coherence level. It displays a behavior similar to the coherence error. So, for a number of sample greater than 50 the error is up to  $1^\circ$  whatever the degree of coherence value within a range from 0.1 to 1. Whilst,  $\sigma_{\phi_z}$  takes the following form:

$$\sigma_{\phi_z} = \frac{2\pi}{Z_a} \sigma_z \quad (9)$$

Finally the errors of estimation which origin from the DEM  $\sigma_{\phi_{DEM}}$  under the forest cover or open area (bared soil) is a function of the height error associated to the DEM  $\sigma_{z_{DEM}}$ . In this work, it was given by the French topographic survey. It is expected that it produces an error on the simulated phase  $\phi_{DEM}$  equal to:

$$\sigma_{\phi_{DEM}} = \frac{2\pi}{Z_a} \sigma_{z_{DEM}} \quad (10)$$

The combination of the equations 5 to 10 yield – by taking into account the main sources of errors – to a global formulation for the errors of estimation of relative and absolute forest cover height as:

$$\sigma_{zrf} = \sqrt{\left[ \sigma_{z_{DEM,forest}}^2 + \sigma_{z_{forest}}^2 \right] + \frac{Z_a}{2\pi} \left( \frac{1-\gamma^2}{N\gamma^2} \right)_{forest}} \quad (11)$$

and

$$\sigma_{zr} = \sqrt{\left[ \sigma_{z_{DEM,forest}}^2 + \sigma_{z_{DEM,soil}}^2 + \sigma_{z_{forest}}^2 + \sigma_{z_{soil}}^2 \right] + \frac{Z_a}{8\pi^2} \left[ \left( \frac{1-\gamma^2}{N\gamma^2} \right)_{forest} + \left( \frac{1-\gamma^2}{N\gamma^2} \right)_{soil} \right]} \quad (12)$$

Within these two equations the left hand side block represents the height variations of the DEM and terrain. The second block focus on the noise of the phase related to the terrain coherence. The relative error will be less than the absolute. Whereas a second source of error – from soil which served as a reference – is added.

### INSAR data

In a first step eleven ERS-1/2 images were selected (Table 1). For the ERS-1 images the acquisitions were realized during the C-phase implying a repeat-pass of the satellite over the area of 35 days. However, during the summer 1995 a tandem phase – couple of ERS-1 and ERS-2 images with one day interval – was programmed by ESA. From there all possible combinations for the baseline (B) and the ambiguity altitude ( $Z_a$ ) were explored. Table 2 presents the results. For ERS-1, the couples with the higher absolute value of  $Z_a$  are cp2-3, cp2-5, cp3-5 and cp4-7. These data

**Table 1. Summary of all the ERS SAR scenes selected over the study site for the interferometric processing.**

Scene	Dates of acquisition	Orbit	Frame	Origin
1	23/04/92	4032	2709	ERS-1 phase C
2	25/08/92	4533	2709	ERS-1 phase C
3	28/01/93	8040	2709	ERS-1 phase C
4	08/04/93	9042	2709	ERS-1 phase C
5	17/06/93	10044	2709	ERS-1 phase C
6	26/08/93	11046	2709	ERS-1 phase C
7	04/11/93	12048	2709	ERS-1 phase C
8	15/07/95	20909	2709	ERS-1 phase G
9	16/07/95	1236	2709	ERS-2
10	19/08/95	21410	2709	ERS-1 phase G
11	20/08/95	1737	2709	ERS-2

**Table 2. Main characteristics of all possible interferometric couples. The couples used for interpretation in this paper are over impressed in grey.**

Couples	1-2	1-3	1-4	1-5	1-6	1-7	2-3	2-4	2-5	2-6	2-7
Baseline (m)	506	392	690	385	758	557	122	1194	125	257	1062
Height of ambiguity (m)	17	23	-13	22	11	-15	-78	-7	-90	33	-8

Couples	3-4	3-5	3-6	3-7	4-5	4-6	4-7	5-6	5-7	6-7	8-9	10-11
Baseline (m)	1077	61	373	944	1072	1440	133	375	940	1308	26	98
Height of ambiguity (m)	-8	590	22	-9	8	6	82	23	-9	-6	-382	109

correspond to different periods which may lead to different states of the forest cover even for coniferous plantations. However, a tandem couple appears also favorable. Here temporal decorrelation effects might have been less.

The interferograms were performed using the DIAPASON estimator (Massonnet 1994) developed by the French Space Agency (CNES – Centre National d'Etudes Spatiales) under a CNES contract. More details on the interferometric processing applied for this study is described in (Castel et al. 2000). For the analysis purpose a GIS-based methodology was developed. The main steps include:

1. The integration of the DEM and interferogram in the GIS;
2. Identification of some homogeneous units to forest (type, structure, height) and topography by the combination of the GIS layers;
3. Extraction of the interferometric signature – computation of the zonal statistics – over the homogeneous units;
4. Calculation of the relative and absolute interferometric height;
5. Comparison of the measured and interferometry-derived forest height,
6. Analysis of the sources of error based on equations 11 and 12.

## RESULTS AND DISCUSSION

### Interferogram image

Figure 3 presents the differential interferogram of the tandem couple cp10-11. A low level of noise is showed over the cause area compared to the other interferogram. Note that higher level of noise arises for foreshortening area – i.e. steep zone – corresponding at the edge of the cause. Smoothing areas appear on the cause by the succession of black and white patches that may be attributed to the wave-like bend of the surface over the plateaus. Following the limits of the forest test site no clear correlation seems to appear between the forest height and the differential phase. However, it is difficult to interpret the interferogram from a first look. Then the analysis of the sensitivity of the phase data – i.e. interferometric derived height – to the measure height was then undertaken.

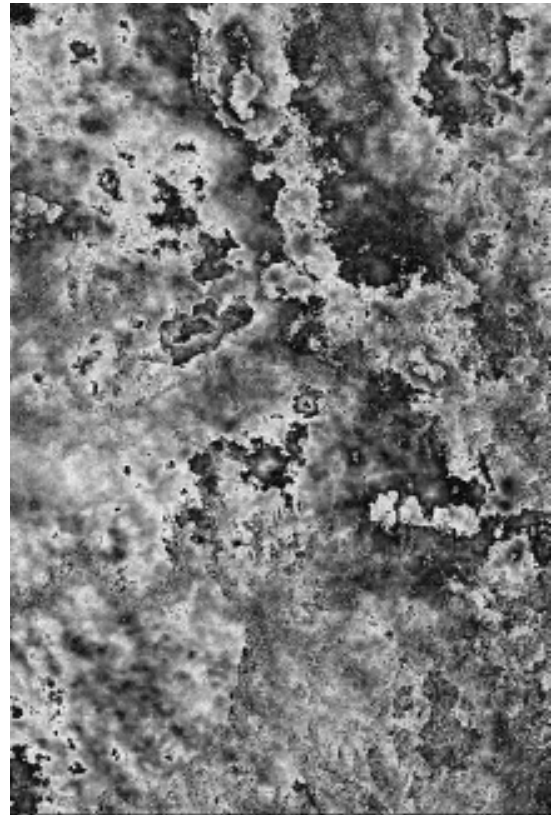


**Fig. 3. Tandem differential interferometer obtained over the whole area. The box indicate the location and limits of the forest study site. A) State forest and B) Privately-owned forest.**

### Experimental sensitivity of the phase to the forest height

Figure 4 shows for the experimental plots the measured height plotted against the interferometry-derived height. This latter was derived from equation 5 and 6. The mean number of independent pixel used for the computation of the phase signature is from 100 to 300. The estimations of the forest height are highly variable whatever the range of the height and the interferometric couple considered. Note that for clarity the results of the couple cp3-5 are not presented. As this couple has the higher height of ambiguity that is larger than those of the other couple comparison purposes

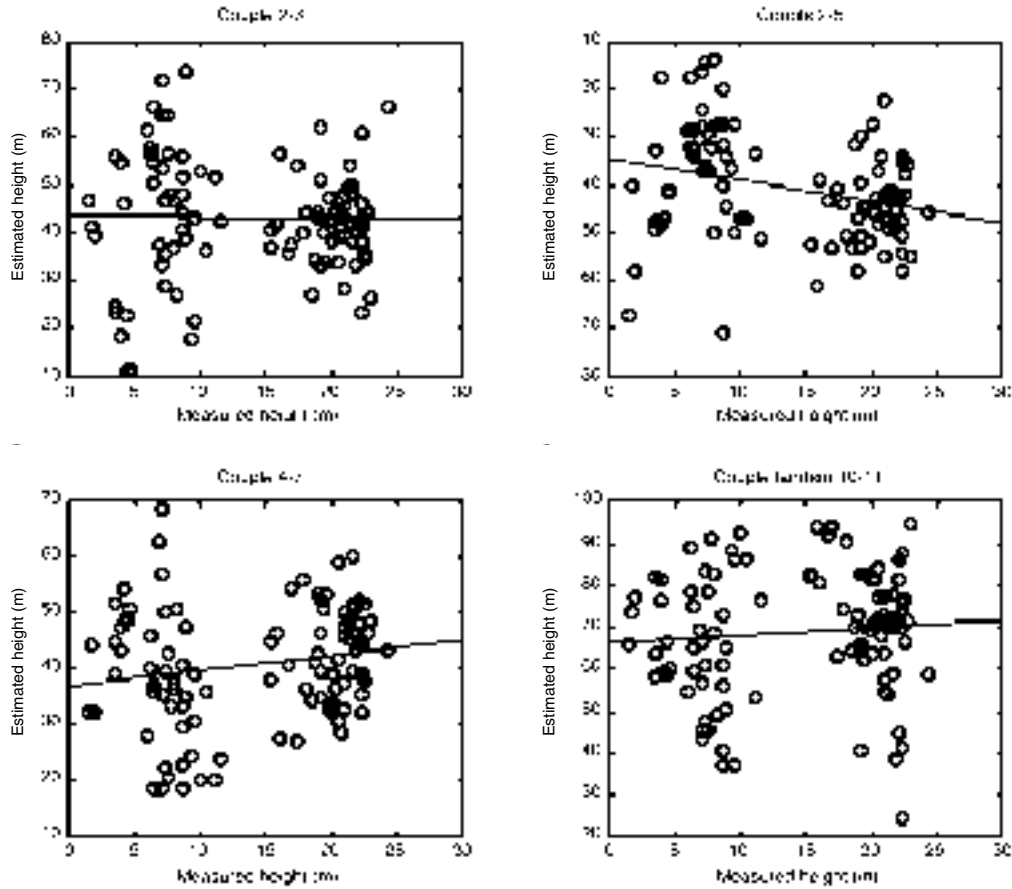


Fig. 4. Field measured forest height vs. interferometric-derived forest height at the homogeneous area level. Interferometric-derived estimates come from the direct transformation of the Digital Number (DN) of the interferogram image.

are difficult to address. No clear trend appears whichever the interferometric couple. A negative height of ambiguity produces a negative variation of the relative residual height. Same type of behavior is obtained for the mean residual absolute height with worst results. Moreover, results may reach to negative height for the forest. As a preliminary conclusion these non conclusive results indicate that such type of data are not currently relevant for the estimation of the forest height.

Hence an explanation of such behavior is needed. For that we have conducted an experimental and theoretical analysis – based on the equation 11 and 12 – to point out the main sources of errors.

**Analysis of the errors**

Table 3 summarizes the various sources of error used to feed the model. From our knowledge as for some of them no data may be obtained a realist range of values was defined. Based on these data a theoretical errors was calculated. The results were compared to the experimental relative and absolute residual errors. Comparisons are given in Table 4. Normally, for bared soil a residual error round zero is expected. Results show that the range of the errors is from 2.2 to 2.7 m while predicted errors is equal to 2.7 m. A satisfactory agreement between measured and simulated errors is reached. Here the main source of error is the uncertainty on the DEM altitude.

Consider now the errors of the relative height over the old forest with mean height from 20 to 23 m. Here the error is high compared to the error for the measured-height which is less than 3 m (see Figure 1). Note that the measured errors take into account the variability inside and among the stands. The simulated-error which includes the variability of the cover height and the DEM uncertainty leads to a value

**Table 3. Sources of errors which affect the estimation of the forest cover height by using the differential interferometric phase.**

Sources of height error	Variable	Standard deviation (m)	Origin
DEM uncertainty, bared soil	$Z_{DEM, soil}$	2.5	IGN
DEM uncertainty, under forest	$Z_{DEM, forest}$	5	Unknown; presume upper than those of soil
Height variability of bared soil	$Z_{soil}$	1	Estimated
Height variability of forest intra-stand	$Z_{forest}$	2 to 3	<i>in situ</i> measurements
Phase noise, bared soil	$\phi_{soil}$	1	Measured coherence (Castel et al. 2000) + equation 8
Phase noise, forest	$\phi_{forest}$	1 to 2, tree height 0 to 25m	Measured coherence (Castel et al. 2000) + equation 8

**Table 4. Measured and predicted mean errors for the bared soil and old forest (Height > 20m). Predicted values within the brackets are calculated with a  $Z_{DEM, forest}$  equal to 7m.**

Couples	Errors, Residual relative height (m)		Errors, Residual absolute height (m)
	Soil	Forest	Forest
2-5	2.2	7.1	13.3
2-3	2.4	6.2	12.6
4-7	2.6	7.9	11.8
10-11	2.7	11.5	13.7
Predicted errors	2.7	6.1 (7.8)	6.7 (8.3)

slightly low compared to the experimental results. Note that the uncertainty of the DEM under the forest cover was taken higher to those of bared soil. Indeed, an arbitrary value of 5 m was fixed for these uncertainty (Table 3). While with a value equal to 7 m the predicted-error rises to 7.8 m which is in close agreement with the observations. Hence the uncertainty of the DEM under the forest cover is the main source of error.

Finally, for the error of the absolute height the uncertainty of the DEM over bared soil and forest area must be considered. A cumulative effect is expected. The results

show very high errors round to the half of the total tree height. Nevertheless predicted error is largely lower than the observed even if the DEM uncertainty under forest rises up to 7 m. Here the most likely explanation comes from 1) the unknown value of the DEM uncertainty and 2) other origins. In particular a systematic error is related to the fact that the scattering center of the layer is not the top of the canopy. An under estimation of the residual height up to 2 m as showed by (Hagberg et al. 1995) systematically arises.

Among the other origin we can restate an important condition which concern the temporal decorrelation – as define by (Zebker and Villasenor 1992) - due to the motions of the scattering elements between the two acquisitions. Indeed, temporal decorrelation precludes the phase comparison of the two images. Temporal decorrelation has been observed over the test site for ERS-1 as well as for tandem interferometric couples (Beaudoin et al. 1996, Castel et al. 2000). For this latter windy conditions produce for the same type of forested areas a roughly drop of the coherence of about 0.3. An under-estimation of this impact by taking only a mean value for the coherence might arisen. By using the equation 11 a numerical experiment was conducted in order to describe and analyze the behavior of the relative height errors as a function of both coherence and height of ambiguity and for three level of  $Z_{DEM}$  under the forest cover.

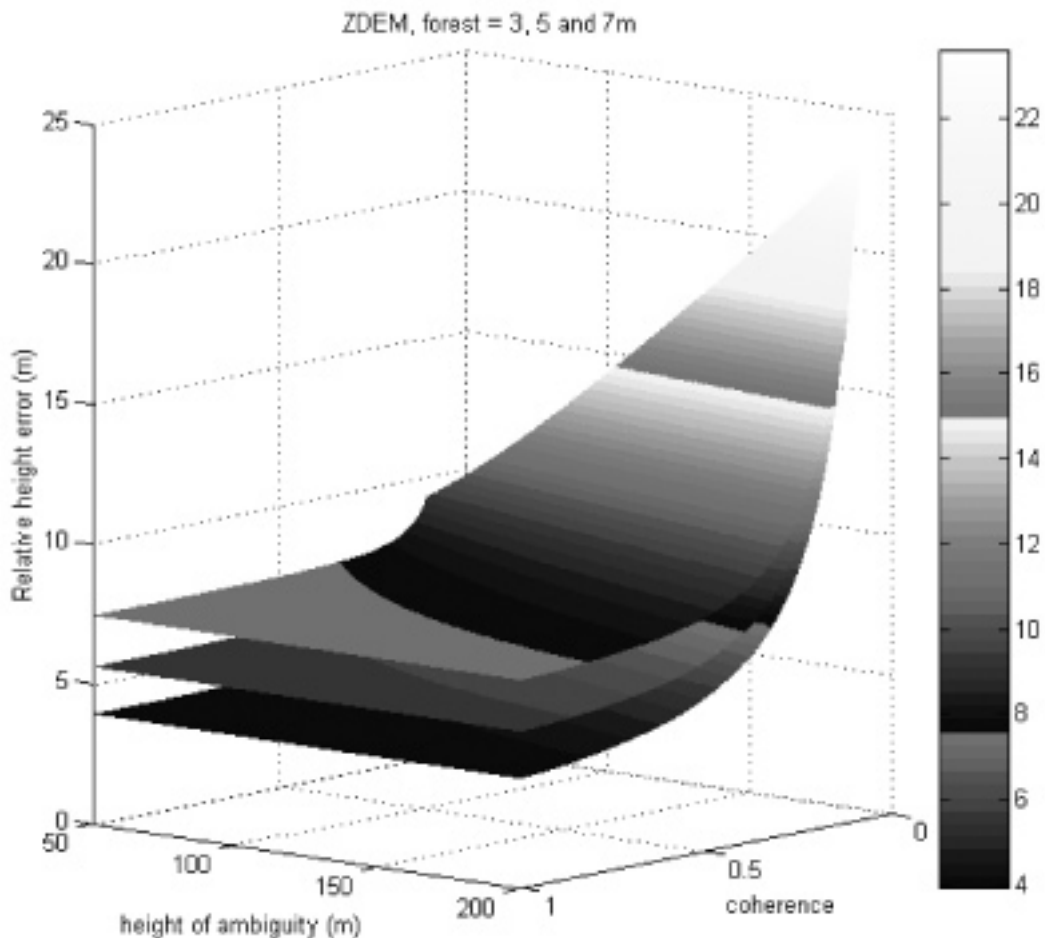


**Fig. 5. Results of the theoretical simulation - based on equation 11 - of the relative height error as a function of both coherence and height of ambiguity and for three values of uncertainty of the DEM under the forest cover. Vertical bar indicates the level of error in meter.**

Figure 5 presents the simulated errors as a 3D surface. Same overall tendency whatever the value of  $Z_{DEM}$  is observed. However, different behaviors arise for low and high coherence values respectively. Indeed, considering first low value of coherence ( $< 0.5$ ), a non linear trend is observed. Here, the effect of the  $Z_{DEM}$  is strongly attenuated and the error is mainly driven by the coherence level. While on an other hand for higher coherence value the opposite case is reached whereas following that the right hand term of equation 11 has a non linear behavior. As a summary, total error displays a threshold – due to the  $Z_{DEM}$  uncertainty – which is modulated by the error related to the coherence level. Similar behavior is reached with the equation of the absolute error. Thus, even for non repeat-pass interferometry minimum source of error remains. Consequently, for application purpose of the differential interferometry technique over forested area a decrease of  $Z_{DEM}$  uncertainty is necessary.

## CONCLUSION

In this study we have established a simple additive model for the estimation of the error on interferometric-derived height based on the use of ERS INSAR data. This model helps us to explain the main source of error when the phase is exercised for the forest height estimation over hilly terrain. Especially for the results of the experimental analysis conducted with the ERS interferogram data acquired over the test area and processed with the CNES DIAPASON software. Indeed, no correlation was obtained between measured and interferometric-derived height. Experimental errors of 8 and 12.8 m were observed for residual relative and absolute height respectively. Hence the results highlight that to date the level of the error of estimation is too strong for the operational use of the differential interferogram for the retrieval of the forest height over hilly terrain. Predicted error was in good agreement for the residual relative height while it under estimates the residual absolute height error. The analysis pointed out that uncertainty on the DEM – particularly under forest cover – is the main source of error. Additional errors whom come from level of coherence and the penetration depth may also be taken into account. The results of the numerical experiment show that the blend of these two sources modulates the total error. However, decorrelation effect drops if the interferogram are generated by a simultaneous acquisition – i.e. using two antennas – from space-borne as well as airborne systems such as SRTM (Shuttle Radar Topography Mission) and TOPSAR (TOPography SAR) systems. Furthermore, theoretical scattering models are powerful tools in order to compensate the under estimation of the interferometric height. Indeed, such model are able to estimate the penetration depth as a function of the forest properties. This was successfully applied by (Floury et al. 1997) for pine plantation over flat area.

By looking the level of error and possible improvements, the estimation of cover height over hilly terrain may concern first forest cover with height greater than 25 m. Furthermore, it may be interesting to examine the non-differential interferogram in order to see if local bounce of the phase is observed with pine plantations. Unfortunately the DIAPASON software is not able to produce such data when the DEM is introduced in the processing chain. Finally if the

use of the differential interferometry is far from forest application over hilly terrain, incoming SAR systems lead to future worthwhile challenge.

## ACKNOWLEDGMENTS

This work was performed within the European project EUFORA and a joint LCT-SCOT project funded by the CNES whom we would like to warmly thank. Particularly Thierry Rabaute and Didier Massonnet for the access to the CNES interferometric processor. Thank also go to ESA for providing the SAR data within a project pilot PP2-F132 and IGN for the DEM.

## REFERENCES

1. Askne J, Dammert PBG and Smith G. Interferometric SAR observations of forested areas. 3rd ERS Symposium. Florence, Italy, 1997; 1-8.
2. Beaudoin A, Le Toan T, Goze S, Nezry E, Lopes A, Mougin E, Hsu CC, Han HC, Kong JA and Shin RT. Retrieval of forest biomass from SAR data. *Int. J. Remote Sens.* 1994;15(14):2777-96.
3. Beaudoin A, Castel T and Rabaute T. Forest monitoring over hilly terrain using ERS INSAR data. *Fringe '96 Workshop*. Zurich, Suisse, 1996 a.
4. Beaudoin A, Castel T and Rabaute T. Potential of ERS1/2 Insar Data for forest monitoring over hilly terrain: case study on Austrian pine plantations. *PIERS 1996*. Innsbruck, Austria, 1996 b.
5. Castel T. Forest biomass retrieval from Synthetic Aperture Radar. Ph. D. Dissertation: ENGREF, Montpellier - France, 1998.
6. Castel T, Martinez JM, Beaudoin A, Wegmüller U and Strozzi T. ERS INSAR data for remote sensing hilly forested area. *Remote Sens. Environ.* 2000;73(1):73-86.
7. Castel T, Caraglio Y, Beaudoin A and Borne F. Using SIR-C SAR data and the AMAP model for forest attributes retrieval and 3D stand simulation. *Remote Sens. Environ.* 2001;75(2):279-90.
8. Dobson MC, Pierce L, Sarabandi K, Ulaby FT and Sharik T. Preliminary analysis of ERS-1 SAR for forest ecosystem studies. *I.E.E.E.T. Geosci. Remote* 1992;30(2):203-11.
9. Dobson MC, Ulaby FT, Pierce LE, Sharik TL, Bergen K, Kellndorfer M, Kendra JR, Li E, Lin YC, Nashashibi A, Sarabandi K and Siqueira P. Estimation of forest biophysical characteristics in northern Michigan with SIR-C/X-SAR. *I.E.E.E.T. Geosci. Remote* 1995;33(4):877-95.
10. Duren R, Wond E, Breckenridge B and Shaffer S. Metrology, attitude and orbit determination for spaceborne interferometric synthetic aperture radar. In: *SPIE, ed. Acquisition, Tracking and Pointing XII*, 1998: 1-10.
11. Evans DL, Plaut JJ and Stofan ER. Overview of the Spaceborne Imaging Radar-C/X-band Synthetic Aperture Radar (SIR-C/X-SAR) missions. *Remote Sens. Environ.* 1997;59:135-40.
12. Floury N, Le Toan T, Souyris JC and Bruniquel J. A study of SAR interferometry over forests: theory and experiment. *Proceedings of IGARSS'97 Symposium*. Singapore, 1997; 1868-70.
13. Gens R and van Genderen JL. Review article: SAR interferometry--issues, techniques, applications. *Int. J. Remote Sens.* 1996;17(10):1803-35.
14. Hagberg JO, Ulander LMH and Askne J. Repeat-pass SAR interferometry over forested terrain. *I.E.E.E.T. Geosci. Remote* 1995;33(2):331-40.
15. Herland EA. SAR interferometry with ERS-1 in forested areas. *Proceedings of IGARSS'95 Symposium*. Florence Italy, 1995: 202-4.
16. Holmes MG. Monitoring vegetation in the future: radar. *Bot. J. Linn. Soc.* 1992;108:93-109.



17. Kasischke ES, Bourgeau-chavez LL, Christensen J, N. L. and Haney E. Observations on the sensitivity of ERS-1 SAR image intensity to changes in aboveground biomass in young loblolly pine forests. *Int. J. Remote Sens.* 1994;15(1):3-16.
18. Kasischke ES, Melack JM and Dobson MC. The use of imaging radars for ecological applications-A review. *Remote Sens. Environ.* 1997;59:141-56.
19. Le Toan T, Beaudoin A, Riou J and Guyon D. Relating forest biomass to SAR data. *I.E.E.E.T. Geosci. Remote* 1992;30(2):403-11.
20. Li FK and Goldstein RM. Studies of multibaseline spaceborne interferometric synthetic aperture radar. *I.E.E.E.T. Geosci. Remote* 1990;28:88-97.
21. Massonnet D and Rabaute T. Radar interferometry: limits and potential. *I.E.E.E.T. Geosci. Remote* 1993;31(2):455-64.
22. Massonnet D, Rossi M, Carmona C, Adragna F, Peltzer G, Feigl K and Rabaute T. The displacement field of the landers earthquake mapped by radar interferometry. *Nature* 1993;364:138-42.
23. Massonnet D. Validation of ERS-1 interferometry at CNES. Second ERS-1 Symposium. Hamburg Germany, 1994; 703-9.
24. Ranson KJ, Saatchi S and Sun G. Boreal forest ecosystem characterization with SIR-C/X-SAR. *I.E.E.E.T. Geosci. Remote* 1995;33(4):867-76.
25. Schmullius CC and Evans DL. Review article: Synthetic aperture radar (SAR) frequency and polarization requirements for applications in ecology, geology, hydrology, and oceanography: a tabular status quo after SIR-C/S-SAR. *Int. J. Remote Sens.* 1997;18(13):2713-22.
26. Ulander L, Dammert PBG and Hagberg JO. Measuring tree height with ERS-1 SAR interferometry. *Proceedings of IGARSS'95 Symposium.* Florence Italy, 1995; 2189-91.
27. Wegmüller U and Werner CL. Farmland monitoring with SAR interferometry. *Proceedings IGARSS'95 Symposium.* Florence, Italy, 1995; 544-6.
28. Wegmüller U, Werner CL and Strozzi T. SAR interferometric and differential interferometric processing chain. *Proceedings IGARSS'98 Symposium.* Seattle, 1998; 1106-8.
29. Zebker HA and Goldstein RM. Topographic mapping from interferometric SAR observations. *J. Geophys. Res.* 1986;91:4993-99.
30. Zebker HA and Villasenor J. Decorrelation in interferometric radar echoes. *I.E.E.E.T. Geosci. Remote* 1992;30(5): 950-9.

*Received July 23, 2001; Accepted in final form January 11, 2002*